Oct 22nd, 12:00 AM

Shell Roofs and Grain Bins Made of Corrugated Steel Sheets

M. N. El-Atrouzy

George Abdel-Sayed

SHELL ROOFS AND GRAIN BINS

MADE OF CORRUGATED STEEL SHEETS

by

M.N. El-Atrouzy[1] and G. Abdel-Sayed[2]

SUMMARY

The paper examines two aspects related to the application of corrugated steel sheets in cylindrical shells. Specifically: a - the type of corrugation appropriate for cylindrical shells, b - grain bins made of corrugated steel sheets.

(1) - Lecturer, Department of Civil Engineering, Ain Shams University, Cairo, Eqypt, formerly, Research Assistant, Department of Civil Engineering, University of Windsor, Windsor, Ontario, Canada

(2) - Associate Professor, Department of Civil Engineering, University of Windsor, Windsor, Ontario, Canada

INTRODUCTION

Cold formed corrugated steel sheets have been subjected to extensive studies, especially in reference to their performance when connected together to form a continuous surface (7). These studies established the basis for the use of steel sheet assemblies as carrying components in structures. The first application of such assembly was in shear diaphragms to replace the shear bracing (8). Next, corrugated sheets with prismatic corrugation were used in folded plate roofs, mainly to carry the shear forces. The flexural tension and compression for such roofs were carried by longitudinal stiffeners (9). In addition, corrugated sheets were used in rectangular hyperbolic paraboloid shells where the applied load is translated into mainly shear forces in the direction of the surface (10).

Corrugated sheets are often produced with cylindrical curvature. These curved sheets are being used in farm buildings and grain bins in spite of the lack of a precise method of analysis. Also, it is generally recognized that cylindrical shells possess good carrying characteristics since they translate the applied loads into mainly membrane forces. Furthermore, it is known that the local buckling strength of curved panels is generally higher than that of plane panels (1, 3).

Therefore, cylindrical shells made of corrugated sheets present an added economical and practical application for the corrugated steel sheets. These applications include such items as long shell roofs, half barrel utility buildings, and grain bins (Fig. 1).

Methods of analysis and economical applications of corrugated steel sheets in cylindrical shells have been presented in a previous paper (2). These analyses are based on treating the shell as being made of elastic orthotropic material in which the mechanical properties are equal to the average properties of the corrugated sheets. This approach was proved through experimentation (1, 5) to be

adequate in considering the main features of response of the shell. The present paper examines additional aspects of these applications in reference to:

a - The type of corrugation to be used in cylindrical shells.

b - Grain bins made of corrugated sheets.

CORRUGATION OF CURVED SHEETS

Cylindrically curved corrugated sheets are widely available with the standard arc-and-tangent type of corrugation (Fig. 2a). The membrane and bending rigidities of these sheets are as follows (4):

$$D_x = \frac{Et}{6(1-\mu^2)} \left(\frac{t}{f}\right)^2 \tag{1a}$$

$$D_\phi = \left(\frac{\ell}{c}\right) Et \tag{1b}$$

$$D_{x\phi} = \rho \frac{Et}{2(1+\mu)} \left(\frac{c}{\ell}\right) \tag{1c}$$

$$B_x = \frac{E\,t^3}{12(1-\mu^2)} \left(\frac{c}{\ell}\right) \tag{1d}$$

$$B_\phi \simeq 0.522\, E\, t\, f^2 \tag{1e}$$

$$B_{x\phi} = \frac{E\,t^3}{12(1+\mu)} \left(\frac{\ell}{c}\right) \tag{1f}$$

in which D_x and D_ϕ = the axial rigidity in the x- and ϕ- directions, respectively; $D_{x\phi}$ = the shear rigidity in the $x\phi$-plane; B_x and B_ϕ = the bending rigidities in the xz- and ϕz-planes, respectively; E = the modulus of elasticity of the material; μ = Poisson's ratio; t = the average thickness of the corrugated sheet; c = corrugation pitch; ℓ = developed length of corrugation per pitch; f = half depth of corrugation; ρ = reduction factor to account for the effect of slip at sheet-to-sheet and sheet-to-stiffeners.

The application of standard arc-and-tangent type of corrugation often requires longitudinal stiffeners at the valleys and crown in shell roofs (Fig. 1b) and vertical stiffeners in grain bins (Fig. 1e). These stiffeners are necessary because of the excessively low membrane rigidity, D_x, in the direction perpendicular to the corrugation, (D_x/D_ϕ is usually about 0.004). This rigidity can be significantly improved as in the two examples outlined below:

(1) A flat plate can be spot welded to the arc-and-tangent type of corrugation (Fig. 2b). The mechanical properties of the sheet become:

$$D_x = \frac{Et_1}{6(1-\mu^2)} \left(\frac{t_1}{f}\right)^2 + Et_2 \tag{2a}$$

$$D_\phi = E\left(t_1 \frac{\ell}{c} + t_2\right) \tag{2b}$$

$$D_{x\phi} = \rho\left[\frac{Et_1}{2(1+\mu)} \left(\frac{c}{\ell}\right) + \frac{Et_2}{2(1+\mu)}\right] \tag{2c}$$

$$B_x = \frac{E}{2}\left[\frac{(t_1+t_2)^3}{12(1-\mu^2)} + \frac{(t_1+t_2)\, f^2}{(1-\mu^2)}\right] \tag{2d}$$

$$B_\phi \simeq E\left(0.522\, f^2 t + 0.0156(1.04\, t_1+t_2)\right) \tag{2e}$$

$$B_{x\phi} = \frac{1.33\, E(t_1+t_2)\, f^2}{2(1+\mu)} \tag{2f}$$

in which t_1 and t_2 = the thickness of the corrugated and flat sheets, respectively.

(2) The arc-and-tangent corrugated sheets can be dimpled as shown in Fig. 2c. This shape was developed recently by Westeel-Rosco of Canada. It possesses higher axial rigidity D_x because of the staggered flat parts which are developed by pressing the originally standard arc-and-tangent type of corrugation. The axial rigidity D_x is determined experimentally. Fig. 3 shows the experimental results which indicate an increase of about 18 times in D_x when compared to its value for the standard type of corrugation, (4). The other membrane and bending rigidities

of the dimpled sheet remain almost the same as for the standard corrugated sheets.

MATHEMATICAL FORMULATIONS:

The differential equations governing the behaviour of orthotropic shells can be written in the form of three simultaneous equations as follows (5):

$$D_x \frac{\partial^2 u}{\partial x^2} + D_{x\phi} \left(\frac{\partial^2 u}{R^2 \partial \phi^2} + \frac{\partial^2 v}{R \partial x \partial \phi}\right) + P_x = 0 \tag{3a}$$

$$D_\phi \left(\frac{\partial^2 v}{\partial \phi^2} - \frac{\partial w}{\partial \phi}\right) + D_{x\phi} \left(R\frac{\partial^2 u}{\partial x \partial \phi} + R^2 \frac{\partial^2 v}{\partial x^2}\right) + R P_\phi = 0 \tag{3b}$$

$$D_\phi \left(\frac{\partial v}{\partial \phi} - w\right) - R^2 B_x \frac{\partial^4 w}{\partial x^4} - 2B_{x\phi} \frac{\partial^4 w}{\partial x^2 \partial \phi^2} - \frac{B_\phi}{R^2} \frac{\partial^4 w}{\partial \phi^2} + R^2 P_z = 0 \tag{3c}$$

in which w, v and u = the displacement in the z-, ϕ- and x-directions, respectively; P_z, P_ϕ and P_x = loading per unit area of the middle surface of the shell in the z-, ϕ- and x- directions, respectively; R = radius of the shell.

The internal force components are calculated in terms of the displacement components as follows:

$$N_x = D_x \frac{\partial u}{\partial x} \tag{4a}$$

$$N_\phi = \frac{D_\phi}{R} \left(\frac{\partial v}{\partial \phi} - w\right) \tag{4b}$$

$$N_{\phi x} = D_{x\phi} \left(\frac{1}{R} \frac{\partial u}{\partial \phi} + \frac{\partial v}{\partial x}\right) \tag{4c}$$

$$M_x = - B_x \frac{\partial^2 w}{\partial x^2} \tag{4d}$$

$$M_\phi = - \frac{B_\phi}{R^2} \frac{\partial^2 w}{\partial \phi^2} \tag{4e}$$

$$M_{x\phi} = M_{\phi x} = - \frac{B_{x\phi}}{R} \frac{\partial^2 w}{\partial x \partial \phi} \tag{4f}$$

in which N_x, N_ϕ = the axial force per unit length acting in the x- and ϕ- directions, respectively; $N_{x\phi}$ = the shear force per unit length acting in the $x\phi$-plane; M_x and M_ϕ = the bending moment per unit length acting in the xz- and ϕz-planes, respectively; $M_{x\phi}$ and $M_{\phi x}$ = the torsional moment per unit length acting about x- and ϕ- axes, respectively.

The governing equations (Eq. 3a, b, c) are based on the classical Donnel approximations. They can be solved in two steps. A membrane solution is obtained for the governing differential equations considering the surface loading. In this solution, the boundary conditions are not satisfied. Thereafter, a bending solution of the governing equations with no surface loading ($P_2 = P_\phi = P_x = 0$) is superimposed in order to satisfy the boundary conditions (5).

A computer program has been written for the IBM system 360/65 for solutions of shells with different boundary conditions. The cases considered are for practical roofs and include single and multiple shells with longitudinal stiffeners in valleys only, and with longitudinal stiffeners in valleys and crowns, as well as half barrels supported along their four edges (5).

APPROXIMATE SOLUTION USING THE BEAM METHOD

The analysis using the differential equations entails considerable calculations and a lengthy computer program. Therefore, it is of particular interest to examine the application of the beam-method which is approximate and easy to apply (6). In addition, the beam method is known to yield reliable results in the case of long shells where the solution based on the differential equations becomes less accurate.

Fig. 4 shows a comparison of the stress resultant N_x at the crown for different ratios of length to radius, L/R, calculated using both the beam-method and the differential equations. It shows that the two solutions become close to

one another at a ratio of L/R ≈ 4.0. Thus for L/R > 4.0, the beam-method provides a reliable method of analysis for shell roofs with the exception of the case when a shell is supported along its four edges.

GRAIN BINS

Grain bins represent a special case of cylindrical shells with rotational symmetry. In this case:

$$P_\phi = N_{x\phi} = Q_\phi = \frac{\partial N_\phi}{\partial \phi} = \frac{\partial M_\phi}{\partial \phi} = M_{x\phi} = 0 \tag{5}$$

Therefore, the governing differential equations, Eq. 3a, b, c, are reduced to:

$$B_x \frac{\partial^4 w}{\partial x^4} + \left(\frac{D\phi}{R^2}\right) w = - P_z \tag{6a}$$

$$\frac{\partial N_x}{\partial x} = - P_x \tag{6b}$$

The lateral pressure P_z can be written in the form:

$$P_z = - K(1 - e^{-\gamma x}) \tag{7a}$$

in which K, γ = constants governed by the properties of the filling material and the dimension of the bin.

The vertical loading:

$$P_x = \chi P_z \tag{7b}$$

in which χ = a constant governed by the friction properties of the filling material and the bin walls. χ is also dependent on the flexibility of the walls of the bin in the vertical direction.

The particular solution for Eq. 6a can be:

$$w_p = \left(\frac{KR^2}{B_x \gamma^4 R^2 + D_\phi}\right) e^{-\gamma x} - \frac{KR^2}{D_\phi} \tag{8a}$$

and the homogeneous solution (5):

$$w_h = e^{-\alpha x}(c_1 \cos\alpha x + c_2 \sin\alpha x) + e^{-\alpha \bar{x}}(c_3 \cos\alpha \bar{x} + c_4 \sin\alpha \bar{x}) \qquad (8b)$$

in which c_1, c_2, c_3 and c_4 = arbitrary constants to be calculated by satisfying the boundary conditions at the upper and lower circular edges of the bin (Fig. 5); $\bar{x} = h - x$; and $\alpha = \sqrt[4]{\frac{D_\phi}{4B_x R^2}}$.

The internal force, N_x, is calculated by simple integration of P_x:

$$N_x = \int_o^x P_x \, dx \qquad (9)$$

Grain bins with no vertical stiffeners may be built using the modified sheets (Figs. 2b, c). Vertical stiffeners are necessary in bins made of standard corrugated sheets (Fig. 2a) or generally if N_x exceeds the allowable value of axial loading (4). In this case, the longitudinal stress resultant N_x becomes unequally distributed throughout the perimeter of the bin. This is due to the shear lag within the sheets leading to maximum stresses at the stiffeners.

To have a ready method for calculation of the maximum stresses and deformations in the bin, the actual width between stiffeners, b_a (Fig. 6), is replaced by an imaginary effective width, b_e. The longitudinal stress resultant, N_x, is assumed to be constant over the width b_e and equal to its maximum magnitude which takes place at the stiffener; thus:

$$b_e = \frac{1}{(N_x)_{max.}} \int_{-b/2R}^{+b/2R} N_x \, R d\phi \qquad (10)$$

The computer program used for shell roofs is employed for the calculation of the actual distribution of N_x. The force P_x is considered to be in the form of a sine wave (Fig. 6). The span of the roof shell is twice the height of the corresponding bin. The lateral section at mid-span of the roof shell represents, approximately, the lower edge of the bin. The conditions along this edge are:

$$u = 0 \qquad N_{x\phi} = 0 \qquad (11a,b)$$

$$\frac{\partial w}{\partial x} = 0 \qquad Q_x = 0 \qquad (11c,d)$$

The supporting edges of the roof shell represents the upper edge of the bin. The conditions along this edge are taken to be:

$$N_x = 0 \qquad v = 0 \qquad (12a,b)$$

$$w = 0 \qquad \frac{\partial^2 w}{\partial x^2} = 0 \qquad (12c,d)$$

These are the conditions at the simply supported upper edge of the grain bin (Fig. 5,b). However the solution for this case is valid also for the case with free upper edge, (Fig. 5b), since it is established, in similar shear lag problems, that the conditions along the transverse end edges have negligible effects on the magnitude of the effective width.

The actual distribution of P_x can be approximated in the form of a single sine wave (Fig. 6) with minor effect on the magnitude of the effective width. In this case, considering a sine wave loading, the effective width, b_e, becomes constant through the height of the bin. The ratio of b_e/b_a is governed only by the ratios of h/b_a and $D_{x\phi}/D_x$.

Fig. 7 is a plotting of $\frac{b_e}{b_a}$ versus $\frac{h}{b_a}$ for a bin made of standard arc-and-tangent corrugated sheet of GA 22.

The vertical stress resultants, N_x, are carried by the stiffeners together with the effective width of the corrugated sheets, i.e. the total area carrying the vertical loading:

$$a_t = \left(b_e \frac{D_x}{E} + a\right) \eta \qquad (13)$$

in which η = number of vertical stiffeners in the bin; a = cross-sectional area of each stiffener.

OBSERVATIONS

1 - The load carrying capacities of shell roofs stiffened at the valleys only, are considerably affected by their type of corrugation. This is illustrated by comparing the maximum allowable span for shell roofs made of:

(a) - Standard arc-and-tangent corrugation (Fig. 2a, GA 18).

(b) - Standard corrugated (GA 24) spot welded to flat plate (GA 24), (Fig. 2b).

(c) - Dimpled arc-and-tangent corrugation (Fig. 2c, GA 18).

Each shell has an average thickness $t \simeq 0.049$, R = 7 ft. $\phi_e = 80^o$ and is subjected to snow loading of 50 psf.

The maximum allowable span, L, is determined for each shell so that the maximum deflection at the crown will not exceed 1/100 of the span and is found to be:

L = 20 ft. for case (a)

L = 70 ft. for case (b)

L = 50 ft. for case (c)

2 - The shear rigidity $D_{x\phi}$ (Eq. 1-c) encounters a reduction factor, ρ to account for the effect of shear slip at sheet-to-sheet and sheet-to-stiffener connection. The effect of this factor on shell roofs and effective width is:

(a) Shell roofs: Fig. 8 shows the percentage of increase in the maximum deflection versus ρ for different L/R ratios. This figure shows that ρ has an insignificant effect on the overall rigidity of the shell. Therefore, the number of shear connectors in the shell should be based only on the strength requirements of the connections.

(b) Effective Width: Because of the shear lag the effective width is less than the actual spacing between the stiffeners. The shear lag is governed mainly by the shear rigidity $D_{x\varphi}$, therefore, ρ has a pronounced effect

on the ratio of b_e/b_a as shown in Fig. 7.

3 - Additional investigations relevant to this subject are being conducted at the University of Windsor. These are:

(a) Modification of the differential equations to achieve a higher degree of accuracy than that obtained when using the equations based on Donnell's assumptions. These equations are of especial importance in the case of shells supported along their four edges since Donnell's equations have a very limited range of validity for t. This study is to be published shortly in the ASCE Journal of Structural Division.

(b) Over-all buckling of the shell roofs subjected to snow and wind loading. This investigation is in progress.

CONCLUSION

The present paper is a further contribution related to the application of corrugated steel sheets in cylindrical shells. It leads to the conclusions:

a - The standard arc-and-tangent type of corrugation can be modified for more appropriate performance in cylindrical shells.

b - The concept of "effective width" is applied to facilitate the calculation of the vertical stress-resultant in grain bins.

APPENDIX I - References

1. Abdel-Sayed, G., "Critical Shear Loading of Curved Panels of Corrugated Sheets", Journal of E. M. Division, ASCE, Dec. 1970, pp. 895-912.

2. Abdel-Sayed, G., El-Atrouzy, M. N., "Cylindrical Shells Made of Corrugated Sheets". International Association of Bridge and Structural Engineering, 1972.

3. Donnell, L. H., "Stability of Thin-Walled Tubes Under Torsion", NACA Report No. 479, 1933, pp. 12.

4. El-Atrouzy, M. N., "Structural Properties of Corrugated Sheets Used in Cylindrical Shells", M.A.Sc. Thesis, University of Windsor, Windsor, Ontario, Canada, 1969.

5. El-Atrouzy, M. N., "Cylindrical Shells Made of Corrugated Sheets", Ph.D. Dissertation, University of Windsor, Windsor, Ontario, Canada, 1972.

6. Lundgren, H., "Cylindrical Shells", The Danish Technical Press, Copenhagen 1960.

7. Luttrell, L. D., "Structural Performance of Light Gage Steel Diaphragms", Report 319, Department of Structural Engineering, Cornell University, August, 1965.

8. Nilson, A. H., "Shear Diaphragms of Light Gage Steel", Journal of the Structural Division, ASCE, Vol. 86, ST11, Nov. 1960.

9. Nilson, A. H., "Folded Plate Structures of Light Gage Steel, ASCE, Transactions, paper No. 3514,(Vol. 128, 1963, Part II), pp. 848-880.

10. Nilson, A. H. "Steel Shell Roof Structures", AISC Engineering Journal, Vol. 3, No. 1, January, 1966.

APPENDIX II - Notation

The following symbols are used in this paper:

B_x, B_ϕ = bending rigidity in xz- and ϕz-planes, respectively;

$B_{x\phi}$ = torsional rigidity;

c = corrugation pitch;

D_x, D_ϕ = axial rigidity in x- and ϕ-directions, respectively;

$D_{x\phi}$ = shear rigidity in xϕ-plane;

E = modulus of elasticity of diaphragm material;

f = half depth of corrugation;

e = developed length of corrugation per pitch;

L = span of shell roof;

M_x, M_ϕ = bending moment per unit length acting in xz- and ϕz-planes, respectively;

$M_{x\phi}$, $M_{\phi x}$ = torsional moment per unit length about ϕ- and x-axis.

N_x, N_ϕ = axial force per unit length acting in x- and ϕ-directions, respectively;

$N_{x\phi}$ = shear force per unit length acting in xϕ-plane;

Q_x, Q_ϕ = lateral shear force per unit length acting perpendicular to x- and ϕ-axis, respectively;

R = radius of shell;

t = average thickness of shell

u,v,w = displacement in x-, ϕ- and z-directions, respectively;

o = reduction factor of shear rigidity;

ν = Poisson's ratio.

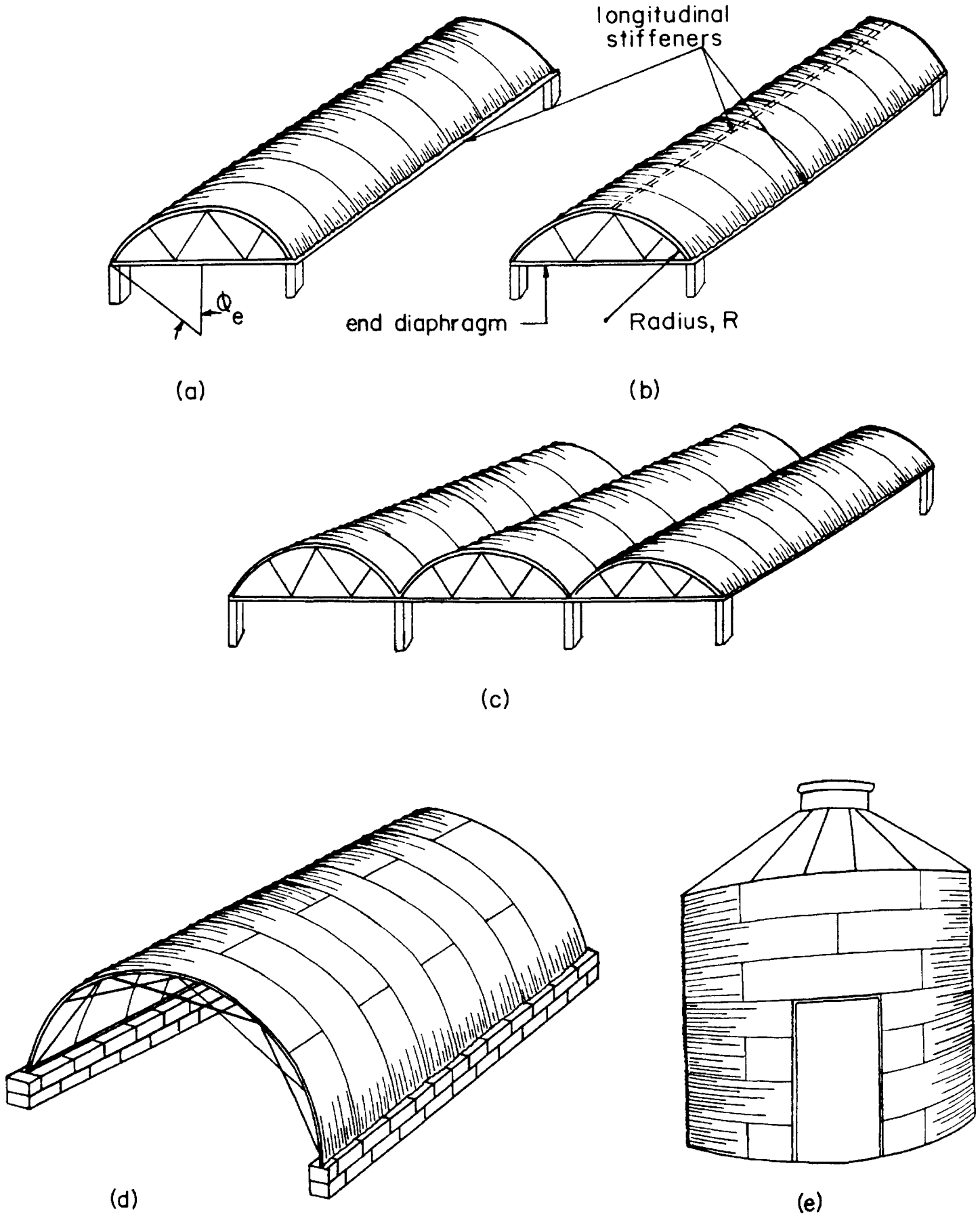

Figure 1: CYLINDRICAL SHELLS
a,b,c = shell roofing
d = utility shelter

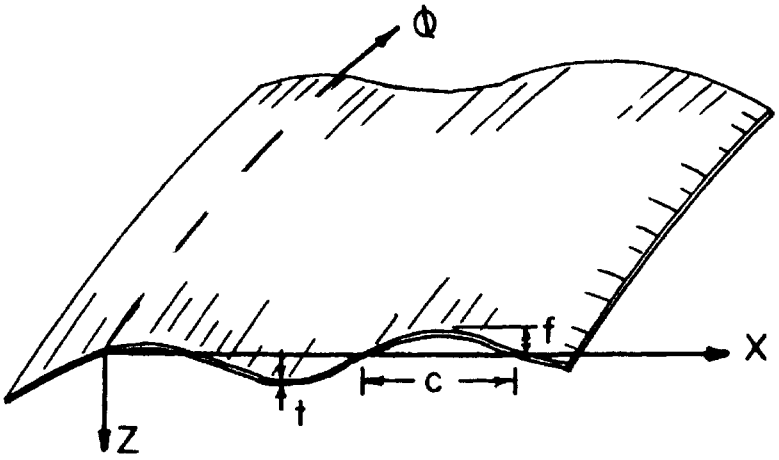

FIG. 2(a): standard corrugation

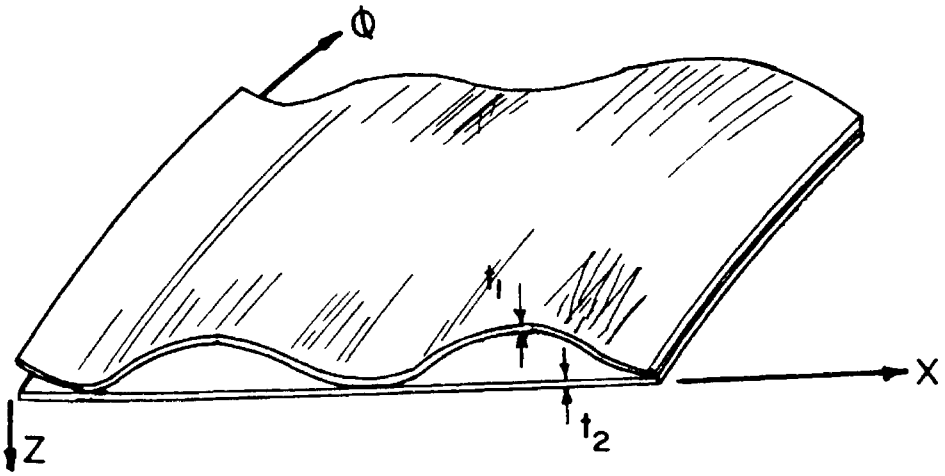

FIG. 2(b): Standard corrugation spot-welded to a plane plate

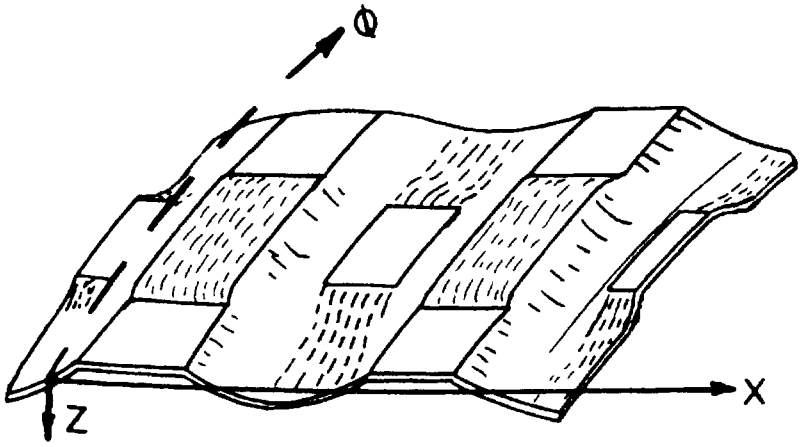

FIG. 2(c): dimpled corrugation

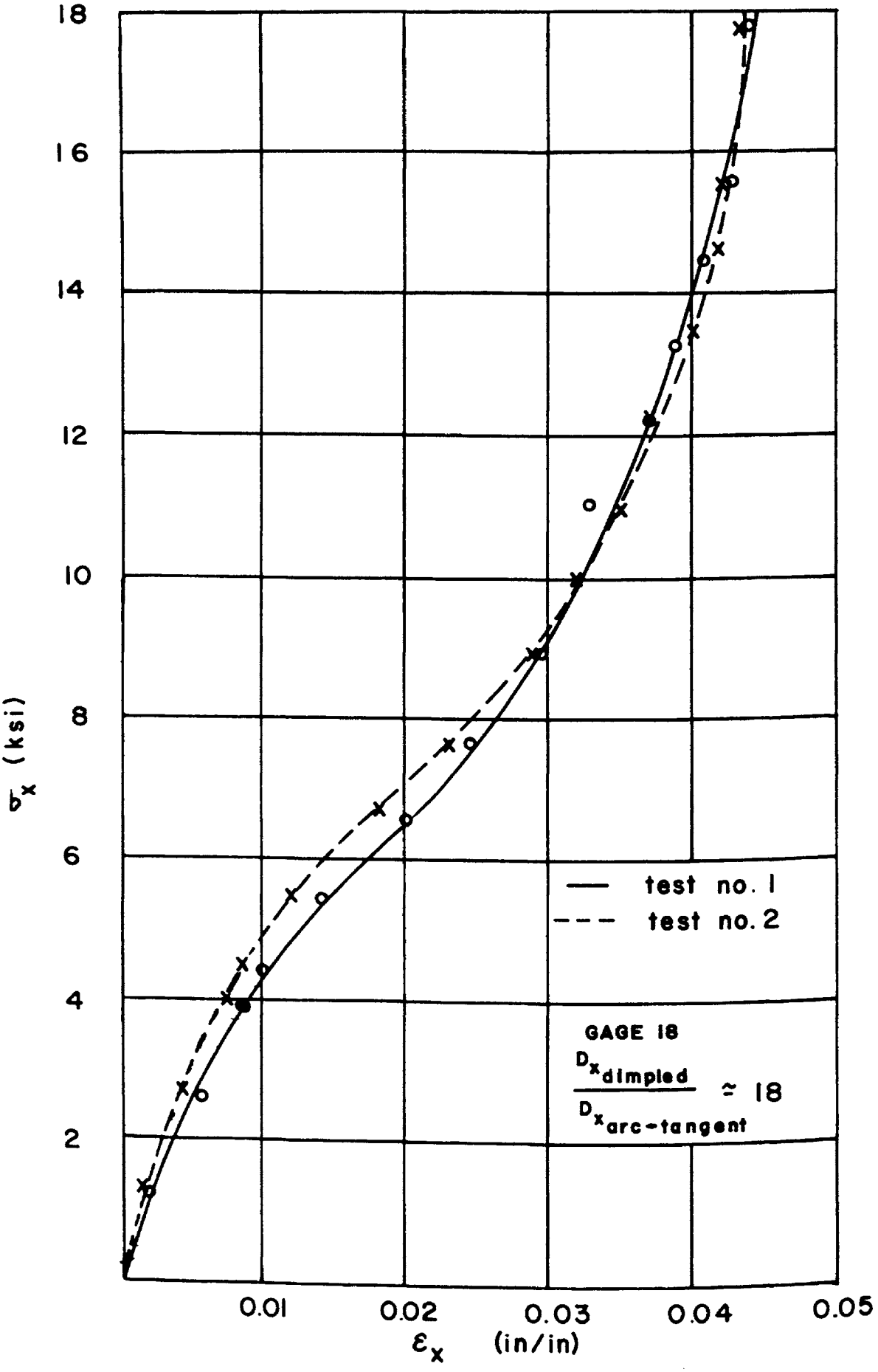

FIGURE 3 : STRESS - STRAIN CURVE OF DIMPLED SHAPE

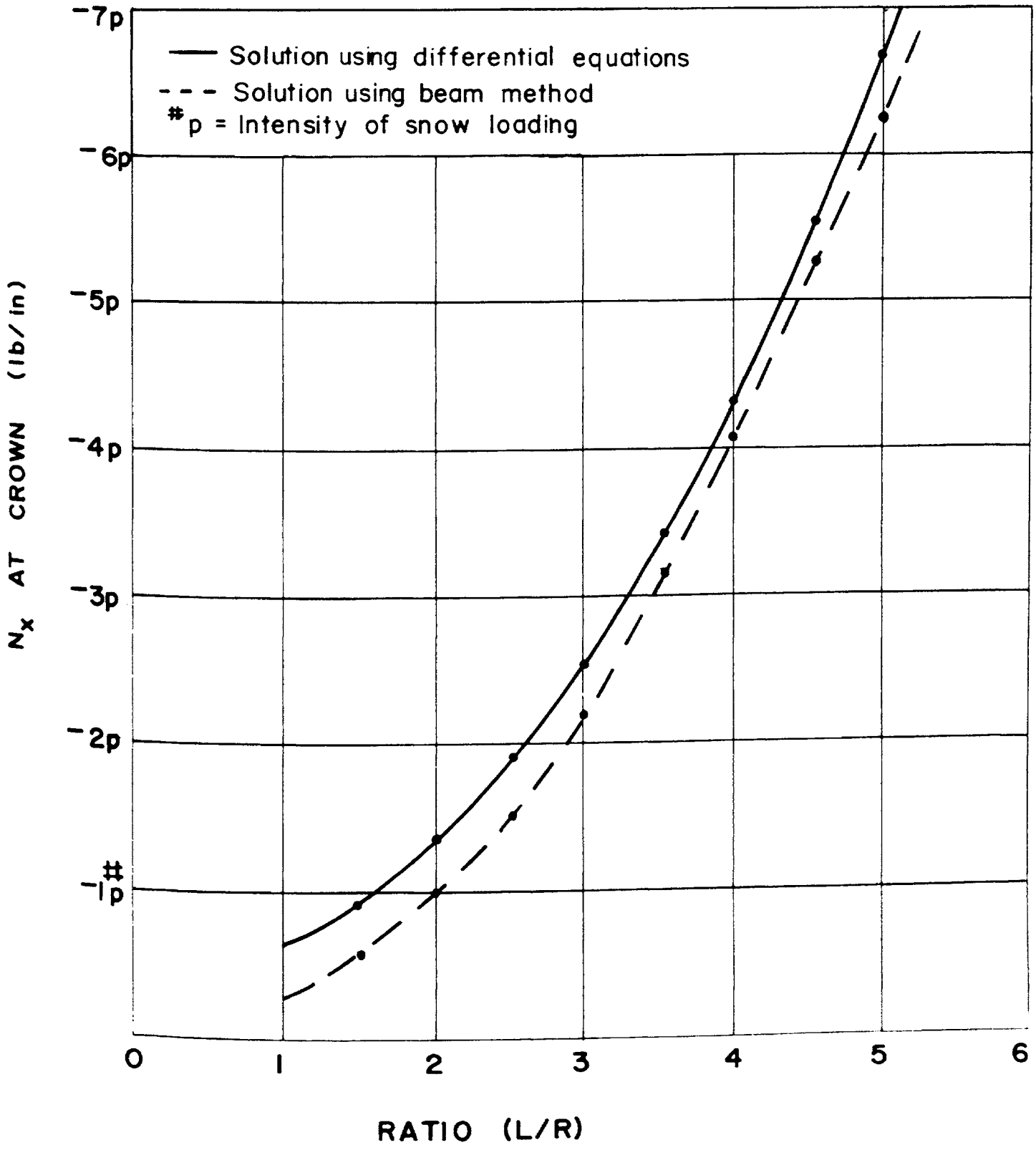

FIGURE (4): COMPARISON BETWEEN SOLUTIONS USING THE DIFFERENTIAL EQUATIONS AND THE BEAM METHOD

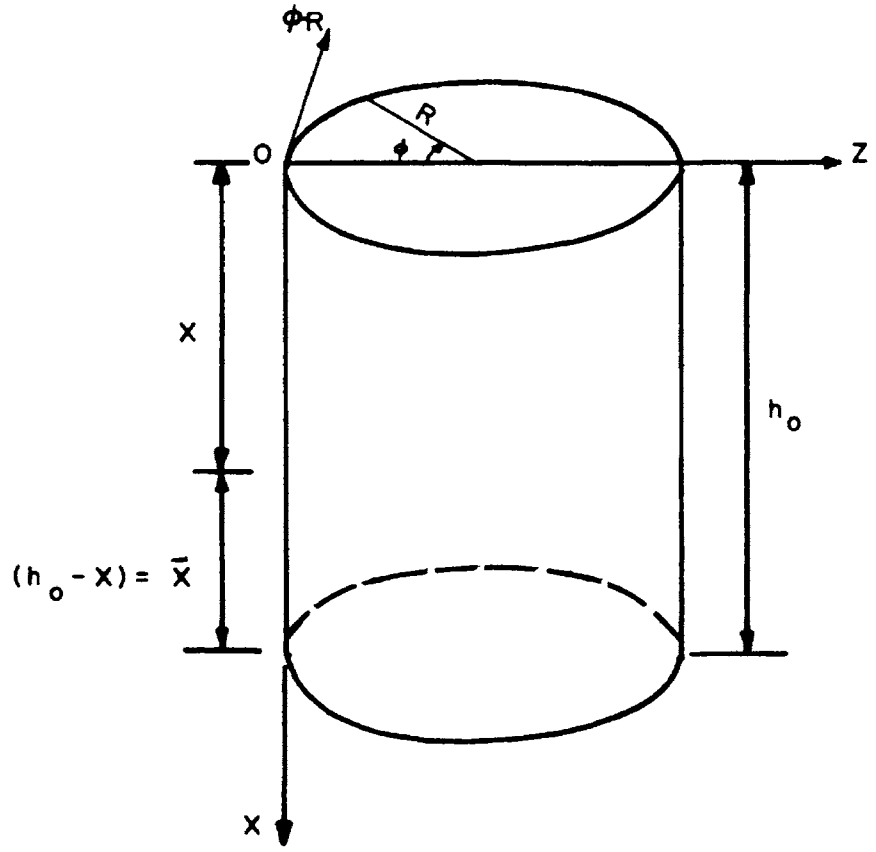

Figure (5-a) : COORDINATE SYSTEM IN GRAIN BINS

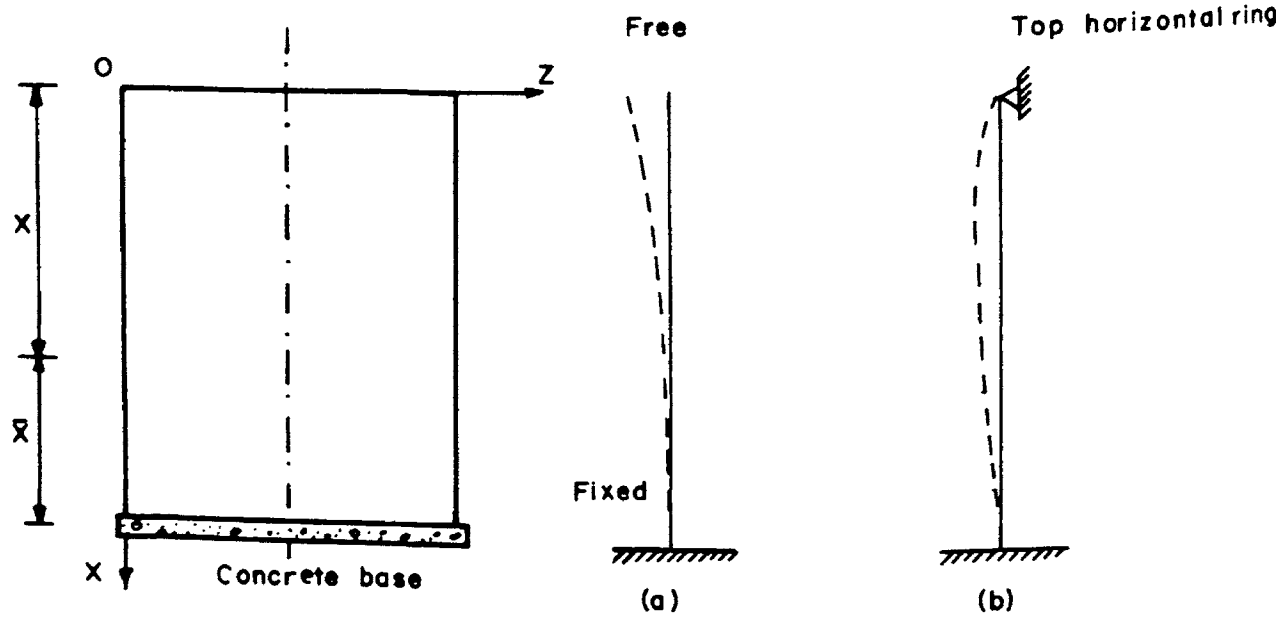

Figure (5-b) : BOUNDARY CONDITIONS IN GRAIN BINS

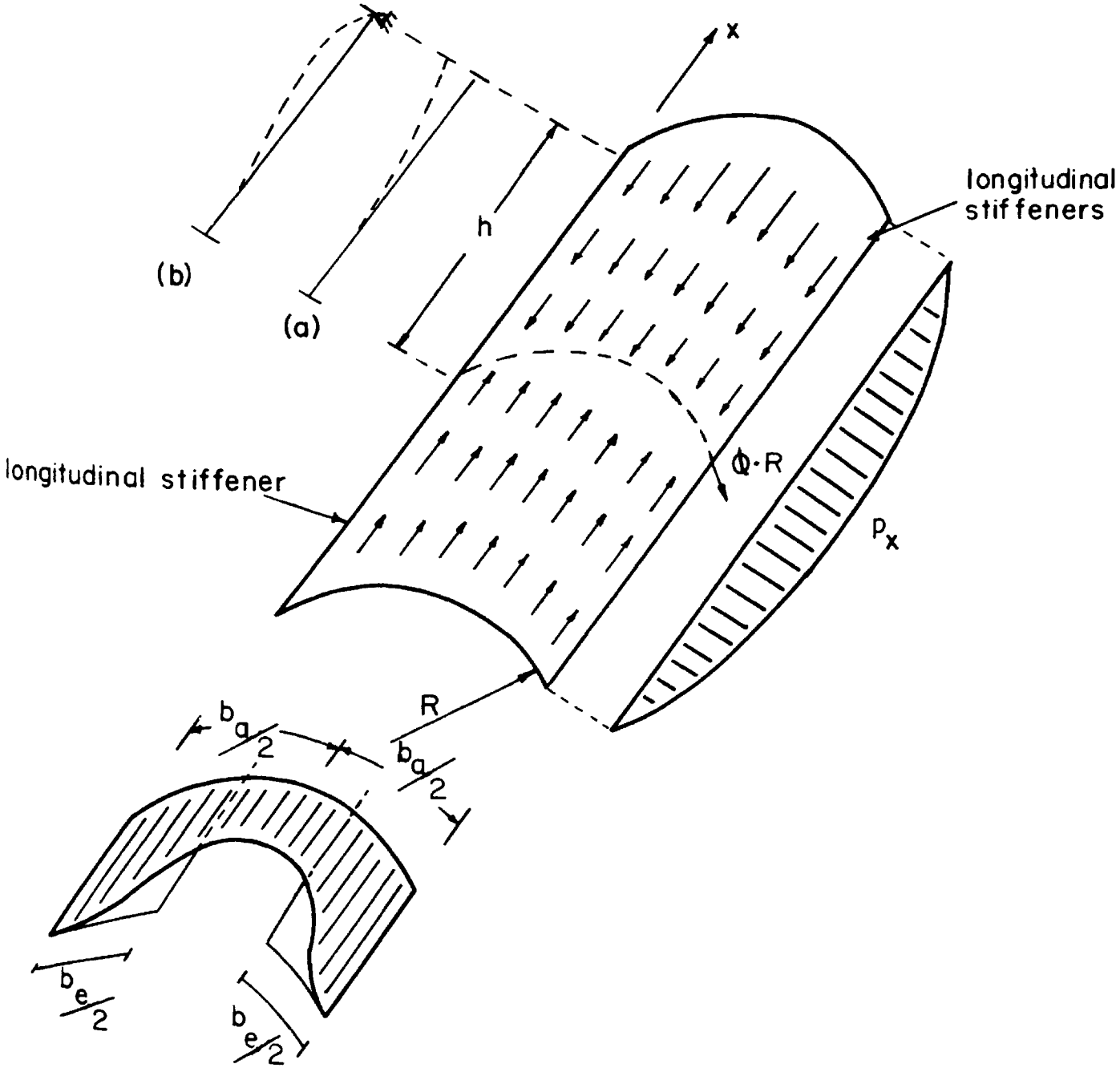
x
h
(b)
(a)
longitudinal stiffeners
longitudinal stiffener
Φ·R
p_x
R
$b_a/2$
$b_a/2$
$b_e/2$
$b_e/2$

Fig. 6

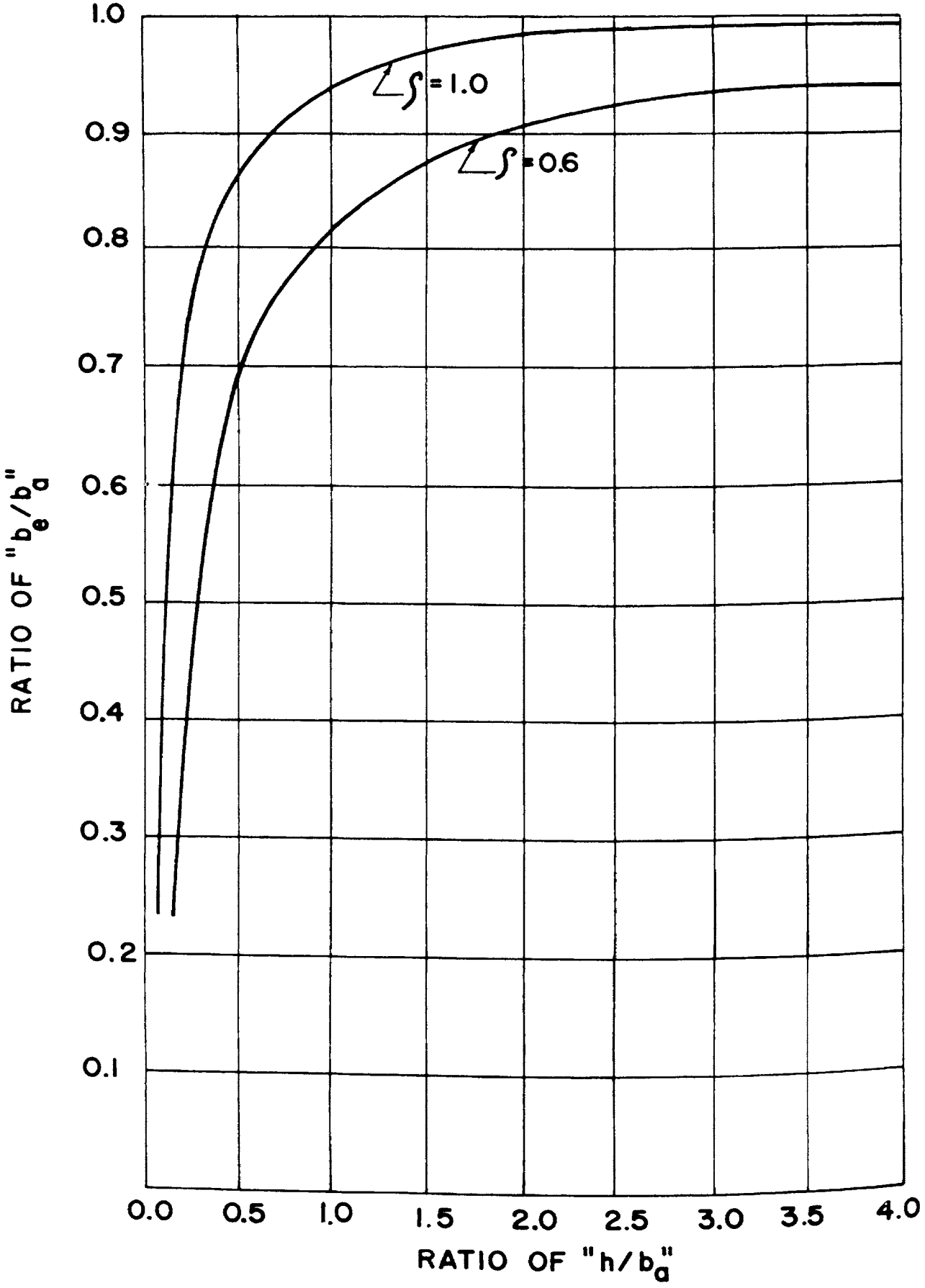

Fig. (7)-EFFECTIVE WIDTH OF CORRUGATED SHEETS

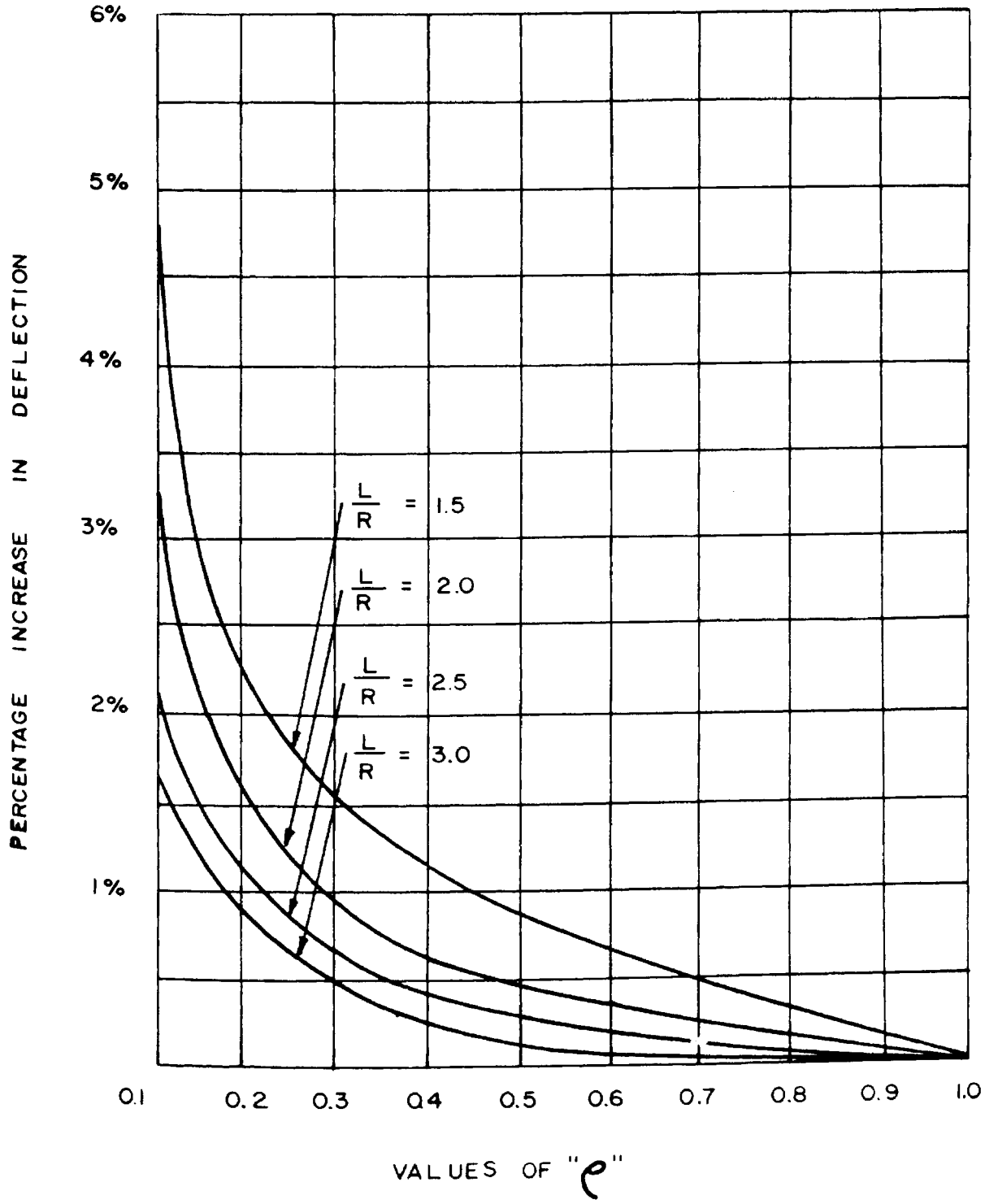

FIGURE (8): EFFECT OF " ρ " ON SHELL ROOFS FOR DIFFERENT RATIOS ($\frac{L}{R}$)